

Boranes

A Highly Effective Ruthenium System for the Catalyzed Dehydrogenative Cyclization of Amine–Boranes to Cyclic Boranes under Mild Conditions

Christopher J. Wallis,^[a, b] Gilles Alcaraz,^{*[a, b]} Alban S. Petit,^[c] Amalia I. Poblador-Bahamonde,^[c] Eric Clot,^[c] Christian Bijani,^[a, b] Laure Vendier,^[a, b] and Sylviane Sabo-Etienne^[a, b]

Abstract: We recently disclosed a new ruthenium-catalyzed dehydrogenative cyclization process (CDC) of diamine–monoboranes leading to cyclic diaminoboranes. In the present study, the CDC reaction has been successfully extended to a larger number of diamine–monoboranes (**4–7**) and to one amine–borane alcohol precursor (**8**). The corresponding NB(H)N- and NB(H)O-containing cyclic diaminoboranes (**12–15**) and oxazaborolidine (**16**) were obtained in good to high yields. Multiple substitution patterns on the starting amine–borane substrates were evaluated and the reaction was also performed with chiral substrates. Efforts have been spent to

understand the mechanism of the ruthenium CDC process. In addition to a computational approach, a strategy enabling the kinetic discrimination on successive events of the catalytic process leading to the formation of the NB(H)N linkage was performed on the six-carbon chain diamine–monoborane **21** and completed with a ¹⁵N NMR study. The long-life bis-σ-borane ruthenium intermediate **23** possessing a reactive NHMe ending was characterized in situ and proved to catalyze the dehydrogenative cyclization of **1**, ascertaining that bis-σ-borane ruthenium complexes are key intermediates in the CDC process.

Introduction

The homogeneous transition-metal-catalyzed dehydrogenation of amine–boranes has produced a wide range of academic research in an attempt to identify suitable catalytic candidates, as well as to determine their mechanism of action.^[1] The dehydrogenation of ammonia–borane, for example, is still regarded as one of the most interesting models for chemical hydrogen storage.^[2] Many effective homogeneous catalytic systems have been discovered, and it is now well established that both the type of the transition-metal catalyst and the nature of the amine–borane unit chosen determine the identity of the product resulting from the dehydrogenation process.^[1b,2] Most systems to date produce the corresponding polymeric aminoboranes, cyclic borazines, and/or polyborazylenes, precursors of BN-containing materials.^[3]

In 2007, we disclosed the unprecedented symmetrical coordination of a monosubstituted borane (RBH₂) to a ruthenium center^[4] involving the geminal σ-B–H bonds of the borane in two three-center two-electron bond interactions with the metal.^[5] Three years later, we reported that the bis(dihydrogen) complex [RuH₂(η²-H₂)₂(PCy₃)₂] (**I**) (Figure 1) led to the stoichiometric dehydrogenation of amine–boranes H₃B–NMe_{3–n}H_n (n = 1–3), at room temperature, with formation of the corresponding bis-σ-B–H aminoborane ruthenium complexes [RuH₂(η²:η²-

[a] Dr. C. J. Wallis, Dr. G. Alcaraz, Dr. C. Bijani, Dr. L. Vendier, Dr. S. Sabo-Etienne
CNRS, LCC (Laboratoire de Chimie de Coordination),
205 route de Narbonne, BP 44099, 31077 Toulouse Cedex 4 (France)
E-mail: gilles.alcaraz@lcc-toulouse.fr

[b] Dr. C. J. Wallis, Dr. G. Alcaraz, Dr. C. Bijani, Dr. L. Vendier, Dr. S. Sabo-Etienne
Université de Toulouse, UPS, INPT, 31077 Toulouse Cedex 4 (France)

[c] Dr. A. S. Petit, Dr. A. I. Poblador-Bahamonde, Dr. E. Clot
Institut Charles Gerhardt, Université de Montpellier,
CNRS 5253, cc 1501, Place Eugène Bataillon,
34095 Montpellier Cedex 5 (France)

Supporting information for this article is available on the WWW under <http://dx.doi.org/10.1002/chem.201501569>.

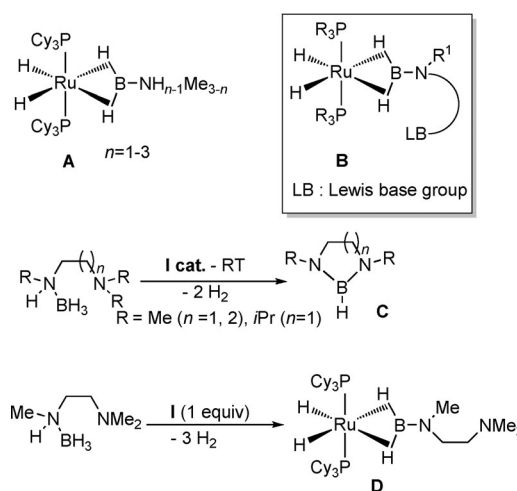


Figure 1. Stoichiometric and catalytic ruthenium dehydrogenation of amine–boranes.

$\text{H}_2\text{BNH}_{n-1}\text{Me}_{3-n}(\text{PCy}_3)_2$] (**A**) (Figure 1).^[6] We clearly showed 1) the ability of ruthenium to retain the B–N unit along the elementary steps of the amine–borane dehydrogenation pathways, and 2) the bis- σ -B–H coordination mode to be a useful tool for the stabilization of monomeric aminoboranes in the coordination sphere of the metal,^[7] enabling even the trapping of the simplest and elusive prototypical $\text{H}_2\text{B}-\text{NH}_2$ elementary unit (Figure 1).^[1a,6]

As a part of our research program focusing on B–H bond activation, we were interested to further explore the reactivity of the bis- σ -B–H coordination mode, based on an approach reminiscent of the intramolecular heterolytic cleavage process of H_2 taking place in the first coordination sphere of a metal in the presence of a nucleophile.^[8] We were particularly interested in investigating the potential intramolecular interaction of the activated σ -bound B–H units towards a Lewis base (LB) moiety located away from the nitrogen atom of the aminoborane unit (**B**). We found that diamine–monoboranes possessing a secondary amine end group were converted into the corresponding cyclic diaminoborane **C** through a catalyzed dehydrogenative cyclization (CDC) process with **I** as a catalyst precursor (Figure 1).^[9] In the case of a pendant tertiary amine group, no cyclization occurred; the reaction was stoichiometric, producing solely the bis- σ -B–H aminoborane ruthenium complex **D**^[9] (Figure 1). Because the outcome of the reaction is influenced by the substitution pattern of the remote amine group, a deeper investigation of the reactivity of a series of diversely functionalized amine–boranes was undertaken. The aim is to better delineate the synthetic potential of this reaction and to provide mechanistic insights, in the continuation of our preliminary results.

Results and Discussion

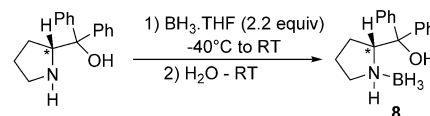
We have already disclosed the ability of $[\text{RuH}_2(\eta^2\text{-H}_2)_2(\text{PCy}_3)_2]$ (**I**) to be a highly effective and robust catalyst for the CDC transformation of three diamine–monoboranes into their cyclic diaminoborane derivatives (Table 1, entries 1–3). Our efforts here focus on expanding the substrate scope and showing the versatile nature of the catalyst towards a variety of substrates. The diamine–monoborane substrates 1–7 (Table 1) used for the catalytic studies were synthesized by the stoichiometric reaction of $\text{BH}_3\text{-SMe}_2$ with the corresponding diamine at -78°C in THF. The products were mostly isolated as colorless oils and fully characterized by NMR spectroscopy. Compounds **6** and **7**, synthesized from the starting enantiopure diamines, were obtained in a 9:1 diastereoisomeric integration ratio due to the presence of a chiral nitrogen atom generated by quaternization with BH_3 .

Synthesis of **8** was performed from the enantiopure (*S*)-(–)- α,α -diphenyl-2-pyrrolidinemethanol by adding two equivalents of $\text{BH}_3\text{-THF}$ followed by a hydrolytic work-up to restore the alcohol moiety while still guarding the amine–borane group (Scheme 1).^[10]

By using the same reported conditions,^[9] the CDC reactions were conducted with substrate 1–8 in THF, in the presence of a 2.5 mol% of **I** as a catalyst (Table 1).

Table 1. Ruthenium CDC of amine–borane substrates.				
Entry	Substrate	Product	<i>t</i> [h] ^[b]	Yield [%] ^[c]
1 ^[a]			3	25
2 ^[a]			8	55
3 ^[a]			3	25
4			16	88
5			72	72
6			30	78
7			30	78
8 ^[d]			24	42

[a] See previous communication.^[9] [b] Time for 100% conversion of the substrate determined by ¹¹B NMR spectroscopy. [c] Yield of the isolated product. [d] Monomer–dimer equilibrium observed for **16**.^[11]



Scheme 1. Synthesis of substrate **8**.

Substrates **4** and **5** were chosen to further evaluate the influence of the steric bulk of the substituent on the nitrogen atoms. The change from a methyl to an isopropyl group had already been shown to more than double the reaction time, from 3 to 8 h (Table 1, entries 1 and 2). Thus, increasing further the steric bulk to a *tert*-butyl group accordingly increases the reaction time to 16 h (Table 1, entry 4). Surprisingly, however, the benzyl-substituted substrate (Table 1, entry 5), which is sterically less encumbered than the *tert*-butyl analogue, does not follow the same correlation, with a 72 h long CDC reaction time for 100% conversion. We speculate that the increased reaction time could be due to the weaker basicity of the *N*-benzyl-substituted amine end group.^[12] In the case of diamine–monoboranes **6** and **7**, the CDC transformation took 30 h to reach complete consumption of substrate, highlighting the influence of the backbone rigidity in the cyclization process for these substrates. The corresponding diazaborolidines

14 and **15** were isolated in 78% yield and one single signal was observed, respectively, in the ^{11}B NMR spectrum. The specific optical rotation for each diazaborolidine was determined (**14**: $[\alpha]_{\text{D}}^{20} = -354 \pm 9$ ($c = 2.76$, CH_2Cl_2), **15**: $[\alpha]_{\text{D}}^{20} = +352 \pm 9$ ($c = 2.83$, CH_2Cl_2)) clearly showing they are enantiomers and that the chirality is preserved during the process.

To expand the scope of the CDC, we examined the nature of the pendant group by changing the amino group to an alcohol function. Under the same conditions and starting from **8**, the chiral oxazaborolidine **16** was produced cleanly, and showed the reported dynamic behavior in solution with interconversion between its monomeric and dimeric forms at ambient temperature in THF.^[11] With this study, we have illustrated the versatility of complex $[\text{RuH}_2(\eta^2\text{-H}_2)_2(\text{PCy}_3)_2]$ (**I**) for a range of substrates with different steric and electronic properties in CDC transformations. The reactions remain clean when monitored by NMR spectroscopy and the cyclized products were quantitatively obtained and isolated in very good to moderate yields when volatile.

As reported in our previous communication, complex **I** serves as a precatalyst and is also identified as the catalyst resting state of the reaction,^[9] **I** being fully regenerated during the CDC process presumably as a result of evolution of dihydrogen. Despite the absence of observable intermediates,^[13] we speculated the reaction mechanism would involve the initial formation of a corresponding bis- σ -borane ruthenium complex with concomitant or subsequent creation of an interaction between the peripheral ending group and the bis- σ -coordinated borane moiety. In this respect, several scenarios can be envisaged, as depicted in Figure 2, including a Lewis acid–base interaction (**E**), the nucleophilic cleavage of the σ -coordinated B–H bond (**F**) or dihydrogen bonding (**G**)^[14] as the prelude to the final dehydrogenation step.

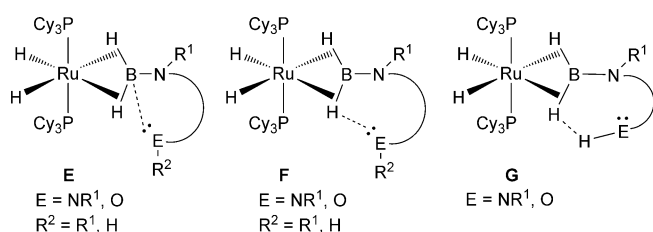


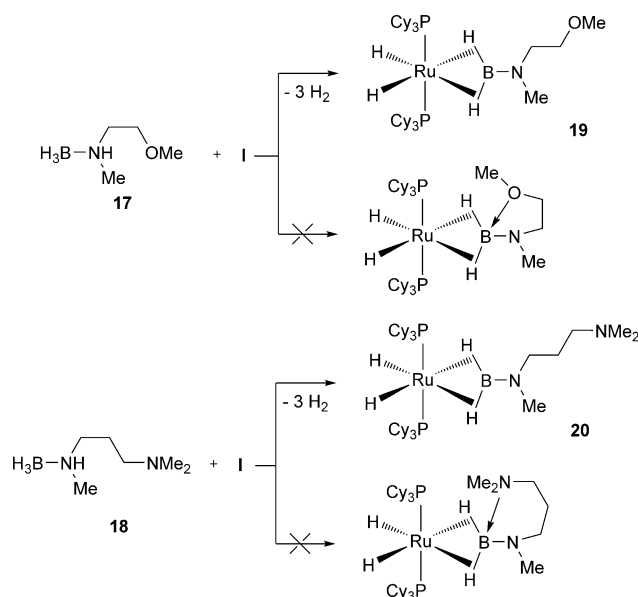
Figure 2. Different scenarios for the final dehydrogenation step in the ruthenium CDC transformation.

Our efforts then focused on trying to isolate the postulated bis- σ -B–H aminoborane-ruthenium complex intermediate in the CDC reaction to track a possible intramolecular interaction as described above. In the preliminary communication, we showed the stoichiometric reaction of *N,N,N'*-trimethylethylenediamine–monoborane with **I** led to the formation of the stable bis- σ -B–H ruthenium complex $[\text{RuH}_2(\eta^2\text{-H}_2\text{BN}(\text{Me})\text{CH}_2\text{CH}_2\text{NMe}_2)(\text{PCy}_3)_2]$ (**D**) (Figure 1). The X-ray diffraction structure showed that the diamine backbone in **D** adopts an open chain structure without any interaction between the pendant NMe_2 group and the ligated borane

moiety, in the solid state. However, the ^1H NMR study of **D** at room temperature in a $[\text{D}_8]\text{THF}$ solution revealed the magnetic nonequivalence of the terminal hydrides ($\delta = -11.94$, -12.27 ppm).^[9] This feature was not observed in the case of the previously reported complex $[\text{RuH}_2((\eta^2\text{-H}_2\text{BNHMe})(\text{PCy}_3)_2)]$ ^[6] with two different substituents attached to the terminal nitrogen atom. This difference is presumably because of a weak barrier to rotation around the B–N bond, rendering the hydrogen atoms surrounding the ruthenium center equivalent. The assumption of an intramolecular interaction increasing the rotational barrier, likely to eliminate magnetic equivalence of the hydride ligands (as depicted in Figure 2), needed to be carefully examined. We checked that point by changing the nature of the peripheral ending group and by modifying the length of the diamine backbone.

The stoichiometric reaction of **I** with amine–borane adducts **17** and **18** led to the corresponding bis- σ -borane ruthenium complexes **19** and **20**, respectively, in high yields (Scheme 2).

The ^1H NMR data were collected and a similar trend was observed for the terminal hydrides in solution at room temperature (**19**: $\delta = -12.12$, -12.40 ; **20**: $\delta = -11.92$, -12.38 ppm). Deeper ^1H NMR investigations of complexes **D**, **19**, and **20** showed each set of signals in the hydride zone, centered at about $\delta = -7$ and -12 ppm, respectively, are averaged upon heating with a decoalescence temperature close to 310 K (see the Supporting Information, Figures S2, S6, and S11). Typically, in the case of **19**, the 2D 1H-EXSY (the Supporting Information, Figure S8) and 2D 1H-ROESY (the Supporting Information, Figure S9) experiments carried out at 243 K showed that the terminal hydrides are exchanging together. The same feature was observed for the boron-bonded hydrides. Consequently, the magnetic nonequivalence observed at room temperature for the four hydrides in these complexes is more probably due to a slow rotation about the B–N bond on the NMR timescale,^[15] than the result of an intramolecular interaction as depicted in



Scheme 2. Synthesis of the bis- σ -borane ruthenium complexes **19** and **20**.

Figure 2. Experimentally, the Eyring and Arrhenius plots of the rate constants (the Supporting Information, Figures S3, S7, and S12) obtained by $^1\text{H}\{^3\text{P};^{11}\text{B}\}$ NMR line shape simulations from the two sets of hydride signals over a significant range of temperature, allowed us to determine a set of thermodynamic parameters ($\Delta G_{\text{coal}}^\ddagger$, ΔH^\ddagger , and ΔS^\ddagger) and to estimate the activation energy (E_a), respectively, for each complex (Table 2). This unprecedented study on the B–N rotational barriers in bis- σ -amino-borane ruthenium complexes is discussed further below.

	E_a [kJ mol $^{-1}$]	ΔH^\ddagger [kJ mol $^{-1}$]	ΔS^\ddagger [J mol $^{-1}$ K $^{-1}$]	G_{coal}^\ddagger [kJ mol $^{-1}$] (at T [K])
D	61.0 \pm 5.4 (BH $_2$) 61.2 \pm 5.2 (RuH $_2$)	58.7 \pm 5.4 58.8 \pm 5.3	–2.5 \pm 19 –2.0 \pm 19	59.4 (298) 59.8 (313)
19	55.3 \pm 3.8 (BH $_2$) 54.9 \pm 2.0 (RuH $_2$)	52.9 \pm 3.7 52.5 \pm 2.0	–21 \pm 13 –22 \pm 5	59.1 (298) 59.1 (308)
20	53.8 \pm 1.7 (BH $_2$) 54.1 \pm 2.4 (RuH $_2$)	51.4 \pm 1.8 51.7 \pm 2.3	–29 \pm 6 –29 \pm 8	60.3 (308) 60.8 (318)
23	51.8 \pm 1.7 (BH $_2$) 52.5 \pm 1.2 (RuH $_2$)	49.4 \pm 1.7 50.0 \pm 1.2	–38 \pm 6 –36 \pm 4	60.8 (308) 61.4 (318)

X-ray crystallography characterization of complexes **19** and **20** (at 110 K) revealed that the peripheral ending groups are again positioned far away from the coordinated borane moiety, in the solid state (Figure 3).

In addition to the amine–borane moiety, the structural requirements of the substrate necessary for the achievement of the CDC transformation include the presence of a remote protic Lewis base. In the absence of any detected intramolecular interaction between the η^2 : η^2 -coordinated BH $_2$ fragment and the methoxy group in **19** or the dimethylamino ending in **D** and **20**, the involvement of a bis- σ borane ruthenium complex as a transient intermediate from which one of the scenarios depicted in Figure 2 could be developed to produce a cyclic diaminoborane, remained questionable. To gain a better insight in this mechanism, we envisioned a strategy that would allow the accumulation and thus the detection of a key catalytic intermediate. We thus turned our attention towards a substrate allowing a kinetic discrimination of the successive events leading to the formation of the NB(H)N linkage. This strategy was conducted by lengthening the carbon chain of the diamine–monoborane to six carbon atoms. We found that **21**, in the presence of 2.5 mol% of **I**, was fully consumed after 48 h at room temperature in [D $_8$]THF. The NB(H)N linkage resulting from the dehydrogenative process was clearly identified with the presence of a characteristic signal at about $\delta = 29$ ppm (**21**: $\delta = -15$ ppm; BH $_3$) for the boron (the Supporting Information, Figure S13) and at $\delta = 3.75$ ppm (**21**: $\delta = 1.49$ ppm; BH $_3$) for the hydrogen atom bonded to boron (the Supporting Information, Figure S14), in the $^{11}\text{B}\{^1\text{H}\}$ and $^1\text{H}\{^{11}\text{B}\}$ NMR spectra, respectively. The presence of a signal at about $\delta = 4$ ppm in the $^{11}\text{B}\{^1\text{H}\}$ NMR spectrum also indicates the presence of cyclodiborazane **22** (Scheme 3) in equilibrium with its monomeric aminoborane form ($\delta = 38$ ppm) upon

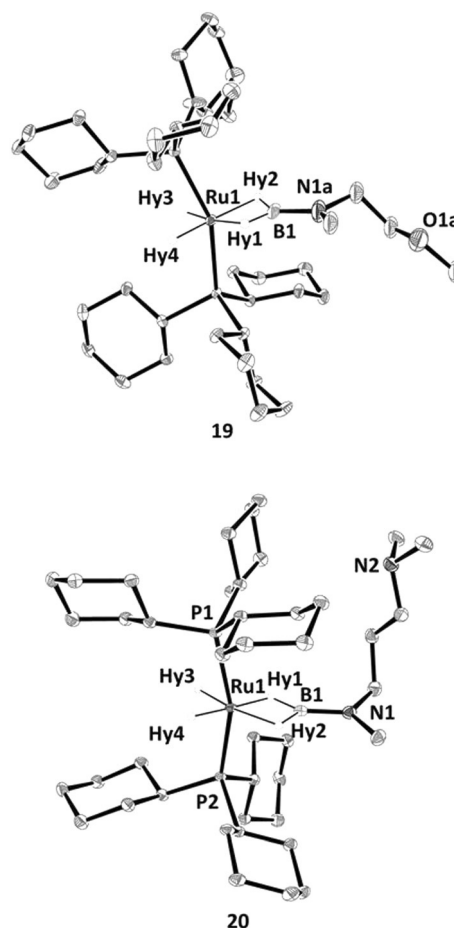
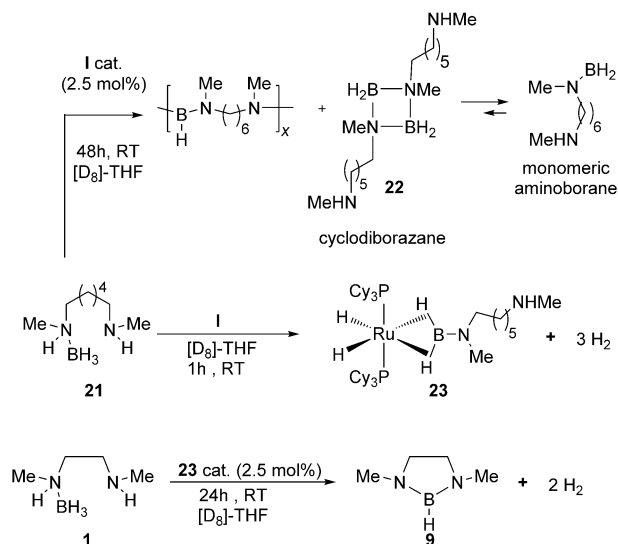


Figure 3. X-ray structures of complexes **19** and **20**. The hydrogen atoms not associated with the metal centers have been omitted for clarity. Ellipsoids set at 30% probability.



Scheme 3. Reaction of diamine-monoboranes **21** and **1** with **I** and **23**, respectively.

heating (the Supporting Information, Figure S15). In the absence of **I**, no dehydrogenation takes place and **21** remained

unchanged after stirring for 5 days in the same conditions. Monitoring the reaction by NMR spectroscopy in the presence of **1** under the reported CDC conditions, we observed the complete consumption of catalyst **1** during the process and the generation of a species resembling a bis- σ -B–H diaminoborane ruthenium complex, which remained at the end of the catalytic process (the Supporting Information, Figures S16 and S17). This result differs quite significantly compared with the other diamine–monoborane substrates for which spectroscopic data suggest that the ruthenium catalyst **1** always remains intact and reusable at the end of the CDC process. To clearly characterize this species, we treated **1** with a sub- or super-stoichiometric amount of **21** at room temperature. Under these conditions, complex **23** could be generated and appeared stable enough to be spectroscopically characterized in solution (Scheme 3). Under super-stoichiometric conditions ($I/21 = 1:1.5$) in $[D_8]THF$ at RT, compound **23** was produced as the major product along with minor amount of the CDC product and traces of cyclodiborazane **22** according to the ^{11}B NMR spectrum (the Supporting Information, Figure S18). The broad signal at $\delta = 47.5$ ppm is consistent with the chemical shifts of previously reported bis- σ -aminoborane ruthenium complexes. The $^{31}P\{^1H\}$ NMR spectrum exhibits two overlapping singlets at $\delta = 79.22$ and 79.20 ppm that split upon heating, presumably as the result of two conformers (the Supporting Information, Figure S19). In the 1H NMR spectrum at 298 K, two sets of signals at $\delta = -7.3$ and -12.7 ppm are observed in the hydride zone in a 1:1 integration ratio (the Supporting Information, Figure S20). The more shielded terminal hydrides and the broad BH signals in **23** are averaged upon heating, allowing the determination of the thermodynamic parameters that are presented in Table 2 (the Supporting Information, Figures S21 and S22). The values obtained for complex **23** are similar to those of **D**, **19**, and **20**. This result is consistent with a slow rotation around the B–N bond on the NMR timescale, exchanging the terminal hydrides, on the one hand, and the BH hydrides on the other.

The activation energy values for these complexes are of similar magnitude (Table 2) but smaller than those for free H_2B-NH_2 , computed to be 141.4 $kJ\ mol^{-1}$ for the rotation barrier with an adjacent trigonal planar nitrogen atom, and 125.1 $kJ\ mol^{-1}$ after relaxation of the nitrogen to a tetrahedral geometry, as the estimation of the π contribution to the B–N bond.^[16] In our study, the rotational barrier is about 50 – 62 $kJ\ mol^{-1}$, and about 80 $kJ\ mol^{-1}$ smaller than that in H_2B-NH_2 , illustrating a reduced B–N π -bonding character in bis- σ -(B–H) aminoborane complexes.

The structure of the transition state for B–N rotation in bis- σ -B–H aminoborane ruthenium complexes should result from a 90° rotation around the B–N bond together with a decrease in the B–N π -bonding, increase in the B–N bond length, and pyramidalization of the nitrogen atom with the lone pair orthogonal to the boron p_z orbital. However, no particular deshielding of boron was observed by ^{11}B NMR spectroscopy for complexes **D** ($\delta = 47.4$ ppm), **19** ($\delta = 47.6$ ppm), **20** ($\delta = 47.4$ ppm), and **23** ($\delta = 47.5$ ppm). This probably results from the synergistic π back-donation from Ru to the empty p orbital

on boron,^[4] together with the donation from the lone pair of the adjacent nitrogen atom.^[7,17] The weakly negative activation entropy value is indicative of a more ordered transition state in the process. These relatively small values are indicative of a dynamic intramolecular process resulting from the rotation around the B–N bond rather than a decoordination–coordination pathway of the aminoborane.

A comparative ^{15}N NMR study of complex **23** with diamine **24**, amine–boranes **21** and **25**, and complex **26**, which possesses a carbon chain of similar length attached to the nitrogen (the Supporting Information, Figures S23–S29), enabled the unambiguous characterization of the pendant NHMe moiety at $\delta = -358$ ppm (Table 3), hence validating the structure of **23** in solution.

Table 3. Comparative study of compounds **21** and **23–26** by ^{15}N NMR spectroscopy.

Compounds	$\delta^{15}N$ [ppm]
21	–351 ($^1J_{15NH} = 67$ Hz) (H_3BNHMe) –357 (NHMe)
23	–299 (H_2BN) –358 (NHMe)
24	–358 (NHMe)
25	–350 ($^1J_{15NH} = 71$ Hz) (H_3BNHMe)
26	–299 (H_2BN)

On that basis, we then showed that the transformation of **1** into **9** was catalyzed by 2.5 mol% of **23** at room temperature (Scheme 3). After 24 h, in addition to the formed diazaborolidine **9**, the presence of **23** was, here again, clearly identified by 1H and $^{31}P\{^1H\}$ NMR spectroscopy, along with traces of **1** generated during the CDC process (the Supporting Information, Figures 30–33).

In light of these results, it seems now realistic to consider the bis- σ -borane ruthenium complexes as likely intermediates in the CDC reaction pathway. The formation of the cyclodiborazane **22** observed at the end of the CDC process from **21** is consistent with this hypothesis. The presence of **22** in solution would result from the displacement of the coordinated aminoborane species by the in situ-generated dihydrogen as a competing ligand at ruthenium, and from its subsequent dimerization in solution (Scheme 3).

DFT (B3PW91) calculations were performed next to obtain insights into the CDC mechanism and the rotational process in the bis- σ adducts (see the Computational Details). The bis- σ complexes **D** and **19** have been computed and the calculated geometries (**D-calc** and **19-calc**) are in excellent agreement with the experimental data (see Table S1 in the Supporting Information). The transition-state structures (**TSrot-D-calc**

and **TSrot-19-calc**) associated with the rotation around the B–N bond have been located on the potential energy surface (PES).^[18] As expected, the transition state corresponds to an almost 90° value for the dihedral angle between the BH₂ plane, which stays coordinated in a bis-σ fashion to Ru, and the NMeR plane (R=CH₂CH₂NMe₂, **TSrot-D-calc**; R=CH₂CH₂OMe, **TSrot-19-calc**).

Upon rotation, the Ru–B bond length decreases by about 0.07 Å and the B–N bond lengthens by about 0.02 Å (Table 4). This is the result of competition of π-donation into the empty p AO on boron from both the occupied d AO on ruthenium and the nitrogen lone pair. In the TS for rotation, the loss of π-donation from nitrogen (longer B–N bond) is compensated by increased π-donation from ruthenium (shorter Ru–B). Interestingly, the hybridization at nitrogen is only slightly altered in the transition state and remains close to trigonal planar (Table 4).

Table 4. Selected geometrical parameters. ^[a]				
	Ru–B	B–N	%p LP(N)	ΔG [‡]
D-calc	1.972	1.407	100	
TSrot-D-calc	1.908	1.424	100	59.6
19-calc	1.971	1.407	100	
TSrot-19-calc	1.904	1.426	99	54.7
DH-calc	1.974	1.404	100	
TSrot-DH-calc	1.905	1.423	99.2	55.8
A1-calc	1.968	1.407	100	
TSrot-A1-calc	1.904	1.431	97	50.7
A2-calc	1.967	1.404	100	
TSrot-A2-calc	1.902	1.432	94.7	39.5
A3-calc	1.957	1.406	100	
TSrot-A3-calc	1.895	1.436	91.3	35.0

[a] Bond lengths [Å] for the bis-σ adducts and the transition state for rotation around the B–N bond, %p character in the lone pair on the nitrogen bonded to boron from NBO analysis, and Gibbs free energy ΔG[‡] [kJ mol⁻¹] of the transition state for rotation around the B–N bond relative to the bis-σ adduct.

The calculated activation barriers ΔG[‡] for the rotation around the B–N bond for **D-calc** and **19-calc** (59.6 and 54.7 kJ mol⁻¹, respectively) are in excellent agreement with the experimental values (Table 2). This lends further credit to the interpretation of the observed exchange process resulting from a rotation around the B–N bond. Calculations on **DH-calc**, an analogue of **D-calc** with a remote NHMe group instead of NMe₂, yielded results very similar with an activation barrier of ΔG[‡] = 55.8 kJ mol⁻¹. In fact, the activation barrier of the rotation around the B–N bond is essentially affected by the nature of the substituents bonded to nitrogen as illustrated by the results for the various bis-σ adducts of H₂BNH_{n-1}Me_{3-n} (**A1-calc**, n=1; **A2-calc**, n=2; **A3-calc**, n=3; see Table 4). When one hydrogen is bonded to N (**A2-calc** and **A3-calc**), the activation barrier for the rotation is significantly reduced and the hybridization at nitrogen changes in the transition state, with more s character in the lone pair resulting in a more pyramidalized nitrogen (Table 4). The value of the rotational barrier, below 40 kJ mol⁻¹, is consistent with fast exchange at room

temperature and, therefore, with the observation of equivalent hydrides.

The NMR experiments and the calculations on the bis-σ adducts did not evidence any significant interaction between the remote Lewis base (NMe₂, NHMe, or OMe) and the boron atom. The experiment with **21** indicated that a bis-σ adduct is an intermediate on the pathway for dehydrogenative cyclization (DC) of amine–borane. However, the experiment with **1** showed that the lifetime of this bis-σ adduct is not long enough to be observed experimentally when the tail is short (here CH₂CH₂NMeH). The bis-σ adduct is thus expected to be formed more slowly than its subsequent transformation to the cyclized product, yet the bis-σ adduct is thermodynamically favored over the bis-dihydrogen starting catalyst. This is confirmed computationally with the bis-σ adduct **DH-calc**, computed to be more stable than [Ru(H)₂(H₂)₂(PCy₃)₂] (**I-calc**) by ΔG = -25.6 kJ mol⁻¹. This complex does not feature any significant interaction between the remote Lewis base NHMe and boron with a B...N distance of 4.257 Å. Isomerization of the CH₂–CH₂–NHMe chain allows to reach several other bis-σ adducts associated to different conformations of the chain. In particular, **DHbend-calc**, featuring a reduced B...N bond length of 3.69 Å is computed to be more stable than that of **DH-calc** by ΔG = -2.9 kJ mol⁻¹ (Figure 4). From **DHbend-calc**, formation of the N–B bond with the remote Lewis base is effective through **TS-BN-calc** with an activation barrier of ΔG[‡] = 71.7 kJ mol⁻¹. The B...N bond length is 2.03 Å in the transition-state structure and the geometry around the boron atom has been altered to accommodate the new bond, as illustrated by the decrease of the Ru–B–N angle from 175.9° in the bis-σ adduct **DHbend-calc** to 141.7° in **TS-BN-calc**. The product of the cyclization, **Prod-BN-calc**, lies at ΔG = 64.7 kJ mol⁻¹ above that of **DHbend-calc** and presents a newly formed B–N bond of 1.752 Å, whereas the already existing B–N bond has been elongated to 1.499 Å. This intermediate can be described as an η²-Shimoi-type bis(σ-amine–borane) complex with one hydrogen atom on one nitrogen.^[19] This protic hydrogen could be engaged in stabilizing interaction with a negatively charged hydride. Indeed, very easy rotation around the Ru...B axis of the 5-membered ring generates, through **TS-Rot-calc**, an intermediate (**Prod-Rot-calc**), featuring a dihydrogen bond between the protic N–H and one hydridic Ru–H (H...H = 1.805 Å).

This transformation has a very low activation barrier of ΔG[‡] = 2 kJ mol⁻¹ and is slightly exoergic (ΔG = -3.4 kJ mol⁻¹). Interestingly, **TS-Rot-calc** not only sets the scene to create a dihydrogen bond, but, in addition, the rotation is accompanied with the cleavage of one B–H bond leading to **Prod-Rot-calc**, that exhibits an elongated B–H bond (B–H = 1.388 Å) and two B–N bonds with a distinct length (1.669 Å vs. 1.450 Å). **Prod-Rot-calc** can be formulated as a borenium ruthenium complex^[20] in which a dihydrogen bond is established with the hydride that was initially bonded to boron. From **Prod-Rot-calc**, a proton transfer from the nitrogen atom to the hydride is effective through **TS-NH-calc** with an activation barrier of ΔG[‡] = 18.5 kJ mol⁻¹. In the TS, the H...H bond length is reduced to 1.105 Å, whereas the N–H bond length is elongated to 1.251 Å (N–H = 1.029 Å in **Prod-Rot-calc**). This N–H bond cleavage is ac-

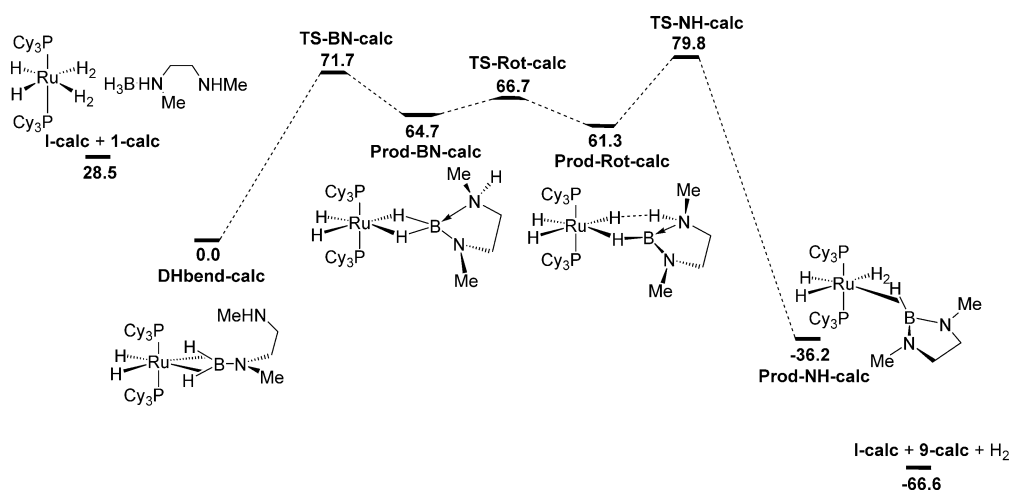


Figure 4. Gibbs free energy profile (kJ mol⁻¹, 298 K) along the pathway for the formation of the cyclic borane from the bis- σ adduct.

accompanied by a shortening of the B...N distance that now becomes closer to the other one (1.579 and 1.431 Å in **TS-Rot-calc** vs. 1.669 Å and 1.450 Å in **Prod-BN-calc**, respectively). The product of the reaction, **Prod-NH-calc**, features a [Ru(H)₂(H₂)(PCy₃)₂] moiety with an η^2 -BH coordination of the product of the DC reaction.

Figure 4 shows the Gibbs free energy profile along the cyclization pathway for the formation of cyclic borane from the bis- σ adduct. This transformation is computed to be strongly exergonic and the substitution of the η^2 -BH bond in **Prod-NH-calc** by a dihydrogen ligand is also energetically favored. The rate-determining step is the N–H cleavage step regenerating a H₂ ligand in the coordination sphere of the metal. From the computed values in Figure 4, formation of the bis- σ adduct **DHbend-calc** from the catalyst **I-calc** and the free aminoborane **1-calc** is computed to be favored energetically.

However, the cyclization process from **DHbend-calc** is very easy, produces the cyclic-borane **9-calc**, and regenerates the catalyst in a strongly exergonic transformation. The activation barrier corresponds to a half-life of the bis- σ adduct of about 10 seconds at 298 K. This is in perfect agreement with the experimental observation in which no bis- σ adduct intermediate could be observed during the CDC reaction, unless the chain is made sufficiently long to retard the B–N bond formation. Also, the η^2 -BH coordination of the cyclic borane is not energetically favored over H₂ coordination, thus explaining why the bis-dihydrogen complex is the resting state of the catalyst.

Conclusion

We have demonstrated that the [RuH₂(η^2 -H₂)(PCy₃)₂] complex (**I**) is an excellent and versatile catalyst for the CDC transformation. It is capable of converting a range of different diamine–monoborane substrates to their cyclic diaminoborane products through a clean process at room temperature. We have also showed that this reaction could be extended to an aminoborane alcohol. The CDC transformation is affected by the steric bulk and the rigidity of the backbone of the diamine–

monoborane substrates, with more sterically encumbered or more rigid backbones causing the CDC process to take more time to reach complete conversion. Exchanging the nature of the peripheral amine unit by a methoxy group or from secondary to tertiary, however, produces solely a stoichiometric reaction. The corresponding complexes **19** and **20** were isolated without any detectable interaction between the peripheral Lewis base moiety and the ruthenium core, neither in the solid state nor in solution. However, characterization of the postulated bis- σ -B–H bound ruthenium aminoborane catalytic intermediate with a reactive NHMe end group was successful by lengthening the carbon chain of the starting diamine–monoborane to six carbon atoms. Using theoretical calculations, and starting from the key intermediate (the bis- σ -B–H aminoborane ruthenium possessing an NHMe dangling moiety), we can propose a cyclization pathway that operates by a stepwise mechanism, resulting from sequential B–H and N–H bond activation. The mechanism involves the successive formation of 1) a η^2 -Shimoi-type bis(σ -amine–borane) complex with a newly formed B–N bond; 2) The stabilization of this complex by B–H bond activation into a σ -B–H borenium ruthenium complex displaying a Ru–H...H–N dihydrogen interaction; Then, 3) N–H bond cleavage leading to the corresponding diaminoborane ligated in a σ -B–H fashion to the ruthenium and further displaced by the produced dihydrogen, thus regenerating the starting bis(dihydrogen) catalyst (**I**).

Investigations with different metal complexes are currently underway to further explore the reactivity of diamine–monoboranes in dehydrogenative processes.

Experimental Section

General methods

All experiments were performed under an atmosphere of dry argon using standard Schlenk and glovebox techniques. Unless stated, all chemicals were purchased from Aldrich and used without further purification. *N,N'*-Di-*tert*-butylethylenediamine, *N,N'*-di-

benzylethylenediamine, *N,N'*-dimethylhexanediamine, and *N,N,N'*-trimethylpropanediamine were dried over calcium hydride and degassed (freeze–pump–thaw) prior to use. $[\text{RuH}_2(\eta^2\text{-H}_2)_2(\text{PCy}_3)_2]$ was prepared according to a literature procedure.^[21] All other solvents were purified and dried through an activated alumina purification system (MBraun SPS-800). NMR solvents were dried using appropriate methods and degassed prior to use. NMR samples of sensitive compounds were prepared under an argon atmosphere. Nuclear magnetic resonance spectra were recorded on Bruker AV300, 400, or 500 spectrometers operating at 300.130, 400.130, or 500.330 MHz, respectively, for ^1H ; 121.495, 161.976, or 202.537 MHz, respectively, for ^{31}P ; 75.468, 100.613, or 125.808 MHz, respectively, for ^{13}C ; 96.293, 128.377, 160.526 MHz, respectively, for ^{11}B ; and 30.420, 40.560 or 50.712 MHz for ^{15}N . ^1H and ^{13}C NMR chemical shifts are reported in ppm referenced internally to residual protio-solvent, whereas ^{31}P , ^{11}B , and ^{15}N NMR chemical shifts were referenced to external 85% H_3PO_4 , $\text{BF}_3\cdot\text{OEt}_2$, and MeNO_2 , respectively. Chemical shifts are quoted in δ (ppm) and coupling constants in Hertz. The following abbreviations are used: br, broad; s, singlet; d, doublet; t, triplet; m, multiplet; ψ , pseudo; app., apparent. Elemental analyses were performed by the “in house” service of the Laboratoire de Chimie de Coordination, Toulouse. Infrared spectra were recorded on a PerkinElmer Spectrum 100 FTIR spectrometer fitted with ATR accessories. The crystal in the ATR module is Ge. Purifications by UPLC were performed by the HPLC service from the ICT (Institut de Chimie de Toulouse) with ultra-performance liquid chromatography (UPLC) system from Waters with a Macherey–Nagel C18 column and a UV detector. High-resolution mass spectra were obtained at the ICT Mass Spectroscopy Service using a Waters Xevo G2 QToF spectrometer using electrospray.

X-ray crystallographic studies

Data for compound **19** and **20** were collected at low temperature (100 K) on a Gemini Agilent diffractometer using a graphite-monochromated $\text{Mo}_{\text{K}\alpha}$ radiation ($\lambda=0.71073 \text{ \AA}$) and equipped with an Oxford Instrument Cooler Device. The final unit cell parameters were obtained by means of a least-squares refinement. The structures have been solved by Direct Methods using SIR92,^[22] and refined by means of least-squares procedures on a F2 with the aid of the program SHELXL97^[23] included in the software package WinGX version 1.63.^[24] The atomic scattering factors were taken from International tables for X-ray Crystallography.^[25] All hydrogen atoms were placed geometrically, and refined by using a riding model, except for the hydrides Hy1, Hy2, Hy3, and Hy4, for both compounds that were located by Fourier differences and isotropically refined. All non-hydrogens atoms were anisotropically refined, and in the last cycles of refinement a weighting scheme was used, in which weights are calculated from the following formula: $w=1/[\sigma^2(\text{Fo})^2 + (\text{aP})^2 + \text{bP}]$ in which $\text{P}=(\text{Fo}^2 + 2\text{Fc}^2)/3$. Drawing of molecule were performed with the program ORTEP32^[26] with 30% probability displacement ellipsoids for non-hydrogen atoms.

Syntheses

Diamine–monoborane 4: $\text{BH}_3\cdot\text{SMe}_2$ (0.55 mL, 1 equiv, 5.8 mmol) through a syringe was added at -78°C to a solution of the *N,N'*-di-*tert*-butylethylenediamine (1.25 mL, 1 equiv, 5.8 mmol) in THF (5 mL). A white precipitate immediately appeared and remained upon warming the reaction mixture to room temperature over 1 h. The reaction mixture was pumped to dryness and the resulting white powder was dried under dynamic vacuum to yield **4** (0.77 mg, 71%). ^1H NMR (C_6D_6 , 400.130 MHz, 298 K): $\delta=4.27$ (brs,

1 H, $\text{N}(\text{BH}_3)\text{H}$), 3.01 (app. qd, 1 H, $J_{\text{HH}}=12.0$, 4.17 Hz, $\text{CH}_2\text{N}(\text{H})\text{BH}_3$), 2.39 (dddd, 1 H, $J_{\text{HH}}=11.2$, 8.7, 3.9, 2.0 Hz, $\text{CH}_2\text{N}(\text{H})\text{BH}_3$), 2.24 (brq, 3 H, BH_3), 2.19 (dddd, 1 H, $J_{\text{HH}}=12.4$, 5.9, 4.0, 2.1 Hz, CH_2NH), 2.09 (app. td, 1 H, $J_{\text{HH}}=11.6$, 4.3 Hz, CH_2NH), 1.08 (s, 9 H, $\text{NC}(\text{CH}_3)_3(\text{H})\text{BH}_3$), 0.86 ppm (m, 1 H, $\text{N}(\text{H})\text{C}(\text{CH}_3)_3$); $^1\text{H}\{^{11}\text{B}\}$ NMR (C_6D_6 , 400.130 MHz, 298 K): $\delta=2.35$ ppm (brs, 3 H, BH_3); $^{13}\text{C}\{^1\text{H}\}$ NMR (C_6D_6 , 100.613 MHz, 298 K): $\delta=57.10$ (s, $\text{NC}(\text{CH}_3)_3(\text{H})\text{BH}_3$), 50.46 (s, $\text{CH}_2\text{N}(\text{H})\text{BH}_3$), 50.38 (s, $\text{N}(\text{H})\text{C}(\text{CH}_3)_3$), 39.02 (s, CH_2NH), 29.54 (s, $\text{NC}(\text{CH}_3)_3(\text{H})\text{BH}_3$), 26.92 ppm (s, $\text{N}(\text{H})\text{C}(\text{CH}_3)_3$); ^{11}B NMR (C_6D_6 , 128.377 MHz, 298 K): $\delta=-19$ ppm (brq, $^1J_{\text{BH}}=97$ Hz).

Diamine–monoborane 5: $\text{BH}_3\cdot\text{SMe}_2$ (0.4 mL, 1 equiv, 4.2 mmol) was added by syringe at -78°C to a solution of the *N,N'*-dibenzylethylenediamine (1 mL, 1 equiv, 4.2 mmol) in THF (5 mL). A white precipitate immediately appeared and remained upon warming the reaction mixture to room temperature over 1 h. The reaction mixture was filtered and the white powder dried under vacuum to yield the bis adduct $[\text{CH}_2\text{NHBz}(\text{BH}_3)]_2$ (54 mg, 10%). The filtrate was pumped to dryness to produce colorless oil. The oil was taken up in toluene (4 mL) and stirred at -40°C for 1 h to remove the diamine starting material. The toluene solution was decanted and then washed with pentane (2×4 mL) at -40°C to yield a colorless oil of **5** (212 mg, 39%). **5:** $^1\text{H}\{^{11}\text{B}\}$ ($[\text{D}_8]\text{THF}$, 500.330 MHz, 298 K): $\delta=7.45\text{--}7.10$ (m, 10H, CH Ar), 5.05 (brs, 1 H, $\text{N}(\text{BH}_3)\text{H}$), 4.12 (dd, 1 H, $^2J_{\text{HH}}=13.6$, $^3J_{\text{HH}}=3.1$ Hz, $\text{PhCHHN}(\text{H})\text{BH}_3$), 3.62 (dd, 1 H, $^2J_{\text{HH}}=13.6$, $^3J_{\text{HH}}=9.6$ Hz, $\text{PhCHHN}(\text{H})\text{BH}_3$), 3.49 (d, 2 H, $^3J_{\text{HH}}=5.0$ Hz, PhCH_2NH), 3.00 (m, 1 H, $\text{CHHN}(\text{H})\text{Bn}$), 2.72 (m, 1 H, $\text{CHHN}(\text{H})\text{BH}_3$), 2.61 (m, 1 H, $\text{CHHN}(\text{H})\text{Bn}$), 2.55 (m, 1 H, $\text{CHHN}(\text{H})\text{Bz}$), 1.75 (1 H, NHbZ), 1.65 ppm (brs, 3 H, BH_3); $^{13}\text{C}\{^1\text{H}\}$ NMR ($[\text{D}_8]\text{THF}$, 125.808 MHz, 298 K): $\delta=141.82$ (s, *ipso*-C PhCH_2NH), 136.53 (s, *ipso*-C $\text{PhCH}_2\text{N}(\text{H})\text{BH}_3$), 130.79 (s, *o*-CH $\text{NHCH}_2\text{Ph}(\text{BH}_3)$), 129.54 (s, *m*-CH $\text{NHCH}_2\text{Ph}(\text{BH}_3)$), 129.05 (s, *p*-CH $\text{NHCH}_2\text{Ph}(\text{BH}_3)$), 129.03 (s, *m*-CH NHCH_2Ph), 128.91 (s, *o*-CH NHCH_2Ph), 127.58 (s, *p*-CH Ar NHCH_2Ph), 60.67 (s, $\text{PhCH}_2\text{N}(\text{H})\text{BH}_3$), 54.03 (s, PhCH_2NH), 53.03 (s, $\text{CH}_2\text{N}(\text{H})\text{BzBH}_3$), 45.66 ppm (s, CH_2NHBz); ^{11}B NMR ($[\text{D}_8]\text{THF}$, 128.4 MHz, 298 K): $\delta=-15$ ppm (brq, $^1J_{\text{BH}}=93$ Hz). Because of the oily nature of **5** at room temperature, no elemental analysis could be properly performed.

Diamine–monoborane 6 and 7: $\text{BH}_3\cdot\text{SMe}_2$ (0.33 mL, 1 equiv, 3.5 mmol) was added by syringe at -78°C to a solution of either enantiopure *R,R*-(-) or *S,S*-(+)-*N,N'*-dimethyl-1,2-cyclohexanediamine (0.5 g, 1 equiv, 3.5 mmol) in THF (4 mL). The reaction solution was allowed to warm to room temperature over 2 h. The reaction mixture was pumped to dryness, which yielded a yellowish oil of **6** (0.336 g, 62%) or **7**, respectively. The product is present in the form of two spectroscopically different diastereoisomers, (ratio of isomers $\approx 90:10$). Major isomer: ^1H NMR (C_6D_6 , 500.330 MHz, 298 K): $\delta=5.55$ (br, 1 H, $\text{NH}(\text{BH}_3)$), 2.61 (app. dt, 1 H, $^3J_{\text{HH}}=4.2$ Hz, $^3J_{\text{HH}}=11.0$ Hz, CHNHMe), 2.11 (s, 3 H, CH_3NH), 2.10 (d, 3 H, $^3J_{\text{HH}}=6.0$ Hz, $\text{CH}_3\text{NH}(\text{BH}_3)$), 1.90 (m, 1 H, CHH), 1.73 (m, 1 H, CHH), 1.61 (m, 1 H, CHH), 1.58 (m, 1 H, CHH), 1.50 (m, 1 H, CHH), 1.39 (m, 2 H, $\text{CHNHMe}(\text{BH}_3)+\text{CHH}$), 0.94 (app. qt, 1 H, $^3J_{\text{HH}}=13.2$ Hz, $^3J_{\text{HH}}=3.6$ Hz, CHH), 0.76 (app. qt, 1 H, $^3J_{\text{HH}}=13.1$, 3.4 Hz, CHHCHNHMe), 0.27 ppm (m, 1 H, CHHCHNHMe); TOCSY $^1\text{H}\{^{11}\text{B}\}$ NMR (C_6D_6 , 500.330 MHz, 298 K): $\delta=2.25$ (s, 3 H, BH_3), -0.5 ppm (br, 1 H, NH); $^{13}\text{C}\{^1\text{H}\}$ NMR (C_6D_6 , 125.808 MHz, 298 K): $\delta=68.31$ (s, $\text{CHNHMe}(\text{BH}_3)$), 58.37 (s, CHNHMe), 41.85 (s, $\text{CH}_3\text{N}(\text{H})\text{BH}_3$), 33.99 (s, CH_3NH), 31.56 (s, CH_2), 25.56 (s, CH_2), 25.33 (s, CH_3), 24.27 ppm (s, CH_2); ^{11}B NMR (C_6D_6 , 128.377 MHz, 298 K): $\delta=-18.4$ ppm (q, $^1J_{\text{BH}}=97$ Hz); Minor isomer $^{13}\text{C}\{^1\text{H}\}$ NMR (C_6D_6 , 125.808 MHz, 298 K): $\delta=66.37$ (s, $\text{CHNHMe}(\text{BH}_3)$), 58.30 (s, CHNHMe), 33.99 (s, $\text{NHCH}_3(\text{BH}_3)$), 33.08 (s, CH_3), 31.03 (s, CH_2), 24.7 (s, CH_2), 24.1 (s, CH_2), 23.92 ppm (s, CH_2); ^{11}B NMR (C_6D_6 , 128.377 MHz, 298 K): $\delta=-14$ ppm (q, $^1J_{\text{BH}}=97$ Hz); Because of the oily nature of **6** and **7** at room temperature, no elemental analysis could be properly performed.

Pyrrolidinemethanol borane adduct 8: A 1 M solution of $\text{BH}_3\cdot\text{THF}$ in THF (1.8 mL, 2 equiv, 1.6 mmol) was added through a syringe to a solution of (*S*)-(–)- α,α -diphenyl-2-pyrrolidinemethanol (200 mg, 0.79 mmol) in THF (10 mL) at -40°C . The reaction mixture was stirred at -40°C for 15 min before H_2O (0.32 mL) was added to quench the excess BH_3 . The mixture was evaporated to dryness and the residue taken up in toluene (10 mL). The toluene solution was dried with MgSO_4 and extracted by filtration and washing with toluene (5 mL). The toluene solution was reduced to a volume of approximately 3 mL, and then placed at -18°C overnight. Compound **8** precipitated as a single diastereoisomer,^[10] affording a white powder that was isolated and dried under vacuum to yield an analytically pure compound (61.5 mg, 29%). ^1H NMR ($[\text{D}_8]\text{THF}$, 400.130 MHz, 298 K): $\delta = 7.62$ (d, 2H, $^3J_{\text{HH}} = 7.2$ Hz, CH Ph), 7.46 (d, 2H, $^3J_{\text{HH}} = 7.8$ Hz, CH Ph), 7.26 (app. q, 4H, $J_{\text{app.}} = 7.5$ Hz, CH Ph), 7.16 (app. q, 2H, $J_{\text{app.}} = 7.1$ Hz, CH Ph), 4.71 (br, 1H, NH), 4.35 (br, 1H, NCH), 3.16 (m, 1H, NCHH), 2.88 (br, 1H, NCHH), 2.14 (m, 1H, NCHCHH), 2.12 (m, 1H, NCH_2CHH), 1.80 (m, 1H, NCH_2CHH), 1.69 ppm (m, 1H, NCHCHH); $^1\text{H}\{^{11}\text{B}\}$ NMR (C_6D_6 , 400.1 MHz, 298 K): $\delta = 2.46$ ppm (br, 3H, BH_3). $^{13}\text{C}\{^1\text{H}\}$ NMR (C_6D_6 , 100.612 MHz, 298 K): $\delta = 144.88$, 144.32 (s, *ipso*-C Ph), 129.18, 128.94, 127.83, 127.01, 126.60 (s, CH Ph), 80.78 (s, Ph_2COH), 72.36 (s, NCH), 55.33 (s, NCH_2), 27.54 (s, NCH_2CH_2), 24.55 ppm (s, NCHCH $_2$); ^{11}B NMR (C_6D_6 , 128.377 MHz, 298 K): $\delta = -12.4$ ppm (br, $^1J_{\text{BH}} = 81$ Hz, BH_3); elemental analysis calcd (%) for $\text{C}_{17}\text{H}_{22}\text{BNO}$: C 76.42, H 8.30, N 5.24; found: C 76.46, H 8.60, N 4.97.

***N,N*-Di-*tert*-butyl-1,3,2-diazaborolidine 12:** $[\text{RuH}_2(\eta^2\text{-H}_2)_2(\text{PCy}_3)_2]$ (2.5 mol%) (14 mg, 0.04 mmol) in THF (4 mL) at room temperature was added to a solution of **4** (0.3 mg, 1.6 mmol) in THF (4 mL). The reaction solution was left to stir at room temperature for 16 h. The volatiles were distilled off through a trap-to-trap distillation under dynamic vacuum. The THF was then separated from the diamino-borane product by a trap-to-trap distillation under reduced vacuum (25°C , 5 millitor) to yield a colorless oil of **12** (0.26 mg, 88%). $^1\text{H}\{^{11}\text{B}\}$ NMR (C_6D_6 , 400.130 MHz, 298 K): $\delta = 4.42$ (s, 1H, BH), 3.13 (s, 4H, CH_2N), 1.18 ppm (s, 18H, $\text{C}(\text{CH}_3)_3$); $^{13}\text{C}\{^1\text{H}\}$ NMR (C_6D_6 , 100.6 MHz, 298 K): $\delta = 50.60$ (s, $\text{C}(\text{CH}_3)_3$), 45.28 (s, CH_2N), 30.59 ppm (s, $\text{C}(\text{CH}_3)_3$); ^{11}B NMR (C_6D_6 , 128.377 MHz, 298 K): $\delta = 26.5$ ppm (d, $^1J_{\text{BH}} = 140$ Hz); IR (neat): $\tilde{\nu} = 2580$ and 2543 cm^{-1} (w, BH); HRMS ESI^+ : m/z calcd for $\text{C}_{10}\text{H}_{24}\text{BN}_2^+$: 182.2069 $[M+\text{H}^+]$; found: 182.2072 (1.6 ppm); exact agreement between the experimental and theoretical isotopic peak distributions, the accurate mass is measured and calculated on the mono-isotopic peak.

***N,N*-Dibenzyl-1,3,2-diazaborolidine 13:** $[\text{RuH}_2(\eta^2\text{-H}_2)_2(\text{PCy}_3)_2]$ (2.5 mol%; 14 mg, 0.03 mmol) in THF (3 mL) at room temperature was added to a solution of **5** (212 mg, 0.83 mmol) in THF (3 mL). The reaction solution was left to stir at room temperature for 72 h, before the solvent was removed under vacuum and the reaction mixture taken up in pentane (4 mL). After filtration and washing with pentane (4 mL), the pentane fraction was reduced to approximately 1 mL and placed at -35°C overnight. The pentane solution was then decanted off and the resulting oil dried under vacuum to yield **13** (151 mg, 72%). ^1H NMR ($[\text{D}_8]\text{THF}$, 400.130 MHz, 298 K): $\delta = 7.33$ – 7.22 (m, 10H, Ar-H), 4.15 (s, 4H, PhCH_2N), 4.08 (br, 3H, BH), 3.07 ppm (s, 4H, CH_2N); $^{13}\text{C}\{^1\text{H}\}$ NMR ($[\text{D}_8]\text{THF}$, 100.613 MHz, 298 K): $\delta = 141.60$ (s, *ipso*-C Ph), 129.16 (s, *m*-CH Ph), 128.46 (s, *o*-CH Ph), 127.59 (s, *p*-CH Ph), 53.03 (s, PhCH_2N), 49.58 ppm (s, $\text{NCH}_2\text{CH}_2\text{N}$); ^{11}B NMR ($[\text{D}_8]\text{THF}$, 128.377 MHz, 298 K): $\delta = 29.4$ ppm (q, $^1J_{\text{BH}} = 129$ Hz); IR (neat): $\tilde{\nu} = 2553$ and 2527 cm^{-1} (w, BH); HRMS ESI^+ : m/z calcd for $\text{C}_{16}\text{H}_{20}\text{BN}_2^+$: 250.1756 $[M+\text{H}^+]$; found: 250.1759 (1.2 ppm), exact agreement between the experimental and theoretical isotopic peak distributions, the accurate mass is measured and calculated on the mono-isotopic peak.

Diazaborolidine 14 and 15: $[\text{RuH}_2(\eta^2\text{-H}_2)_2(\text{PCy}_3)_2]$ (2.5 mol%; 40 mg, 0.06 mmol) in THF (5 mL) at room temperature was added to a solution of either **6** or **7** (370 mg, 0.24 mmol) in THF (5 mL). The reaction solution was left to stir at room temperature for 30 h. The volatiles were distilled off by a trap-to-trap distillation under dynamic vacuum. The THF was then separated from the diamino-borane product by a trap-to-trap distillation under reduced vacuum (5°C , 5 millitor) to yield a colorless oil of **14** or **15** (0.28 mg, 78%). For **14**: $[\alpha]_D^{20} = -354 \pm 9$ ($c = 2.76$, CH_2Cl_2); for **15**: $[\alpha]_D^{20} = +352 \pm 9$ ($c = 2.83$, CH_2Cl_2). $^1\text{H}\{^{11}\text{B}\}$ NMR (C_6D_6 , 400.130 MHz, 298 K): $\delta = 4.24$ (br, 1H, BH), 2.62 (s, 6H, CH_3N), 2.48 (br, 2H, CH), 1.86 (br, 2H, CH_2), 1.59 (br, 2H, CH_2), 1.08 ppm (br, 4H, CH_2); $^{13}\text{C}\{^1\text{H}\}$ NMR (C_6D_6 , 100.625 MHz, 298 K): $\delta = 69.60$ (s, CHN), 32.71 (s, CH_3), 30.01 (s, CH_2), 25.59 ppm (s, NCH_3); ^{11}B NMR (C_6D_6 , 128.377 MHz, 298 K): $\delta = 31.7$ ppm (d, $^1J_{\text{BH}} = 142$ Hz); IR (neat): $\tilde{\nu} = 2541$ and 2507 cm^{-1} (w, BH); HRMS ESI^+ : m/z calcd for $\text{C}_8\text{H}_{18}\text{BN}_2^+$: 152.1599 $[M+\text{H}^+]$; found: 152.1595 (2.6 ppm), exact agreement between the experimental and theoretical isotopic peak distributions, the accurate mass is measured and calculated on the mono-isotopic peak.

Oxazaborolidine 16: $[\text{RuH}_2(\eta^2\text{-H}_2)_2(\text{PCy}_3)_2]$ (2.5 mol%; 3.8 mg, 0.05 μmol) in THF (3 mL) at room temperature was added to a solution of the (*S*)-(–)- α,α -diphenyl-2-pyrrolidinemethanol-mono-borane **8** (58.1 mg, 0.02 mmol) in THF (3 mL). The reaction solution was left to stir at room temperature for 24 h, before the solvent was removed under vacuum and the reaction mixture taken up in toluene (1 mL). Pentane (3 mL) was added and a white powder precipitated. Filtration, then washing with pentane (1 mL), followed by drying under vacuum yielded a white powder analyzed as oxazaborolidine **16** (24.0 mg, 42%), as previously reported in the literature.^[11] Selected data: $^{11}\text{B}\{^1\text{H}\}$ NMR ($[\text{D}_8]\text{THF}$, 128.4 MHz, 298 K): $\delta = 28.4$ (brs), 7.4 ppm (brs).

***N*-(2-Methoxyethyl)methylamine borane adduct 17:** $\text{BH}_3\cdot\text{SMe}_2$ (1 mL, 1 equiv, 10.54 mmol) was added by syringe at room temperature to an ethereal solution of *N*-(2-methoxyethyl)methylamine (1.132 mL, 10.54 mmol). The reaction solution was left to stir at room temperature for 24 h. The mixture was evaporated to dryness to yield **17** quantitatively as colorless oil. ^1H NMR (C_6D_6 , 300.130 MHz, 298 K): $\delta = 3.51$ (brs, 1H, NH), 3.25 (ddd, 1H, $^3J_{\text{HH}} = 10.7$, 7.5, 3.5 Hz, 1H, MeNCHH), 2.89 (s, 3H, OCH $_3$), 2.80 (br, 1H, MeNCHH), 2.56 (m, 1H, CHHOMe), 2.21 (br q, 3H, BH $_3$), 2.12 (m, 1H, CHHOMe), 1.92 ppm (d, 3H, $^3J_{\text{HH}} = 4.6$ Hz, NCH $_3$); $^{13}\text{C}\{^1\text{H}\}$ NMR (C_6D_6 , 75.468 MHz, 298 K): $\delta = 67.54$ (s, OCH $_2$), 58.76 (s, OCH $_3$), 56.54 (s, CH_2N), 42.43 ppm (s, NCH $_3$); ^{11}B NMR (C_6D_6 , 96.293 MHz, 298 K): $\delta = -14$ ppm (q, $^1J_{\text{BH}} = 98$ Hz); Because of the oily nature of **17** at room temperature, no elemental analysis could be properly performed.

Diamine-mono-borane adduct 18: A 1 M solution of $\text{BH}_3\cdot\text{THF}$ in THF (3.4 mL, 1 equiv, 3.4 mmol) was added by syringe at room temperature to a neat solution of *N,N,N'*-trimethylpropanediamine (2 mL, 4 equiv, 14 mmol). The reaction solution was left to stir at room temperature for 24 h. The mixture was evaporated to dryness and re-dissolved in CH_2Cl_2 (10 mL) and passed through a small plug of silica gel. The silica was washed with CH_2Cl_2 (5 mL) and the combined CH_2Cl_2 fractions were pumped to dryness to yield a colorless oil of **18** (193 mg, 43.5%). $^1\text{H}\{^{11}\text{B}\}$ NMR (C_6D_6 , 400.130 MHz, 298 K): $\delta = 5.63$ (brs, 1H, NH), 2.73 (m, 1H, MeN(H)CHH), 2.37 (d, 3H, $^3J_{\text{HH}} = 3.1$ Hz, BH $_3$), 2.07 (d, 3H, $^3J_{\text{HH}} = 6.0$ Hz, $\text{NHCH}_3(\text{BH}_3)$), 2.06 (m, 1H, NCHH), 1.90 (dddd, 1H, $^3J_{\text{HH}} = 12.5$, 6.9, 3.7, 0.8 Hz, NCHH), 1.83 (s, 6H, $\text{N}(\text{CH}_3)_2$), 1.80 (m, 1H, NCHH) 1.60 (m, 1H, NCH_2CHH), 0.98 ppm (dt, 1H, $^3J_{\text{HH}} = 15.2$, 7.1, 3.6 Hz, NCH_2CHH); $^{13}\text{C}\{^1\text{H}\}$ NMR (C_6D_6 , 100.613 MHz, 298 K): $\delta = 60.27$ (s, NCH $_2$), 58.92 (s, NCH $_2$), 45.53 (s, $\text{N}(\text{CH}_3)_2$), 42.61 (s, CH_3) 22.44 ppm (s, NCH_2CH_2); ^{11}B NMR

(C_6D_6 , 128.377 MHz, 298 K): $\delta = -14$ ppm (q, $^1J_{BH} = 96.5$ Hz). Because of the oily nature of **18** at room temperature, no elemental analysis could be properly performed.

Complex 19: A solution of $[RuH_2(\eta^2-H_2)(PCy_3)_2]$ (100 mg, 0.01 mmol) in toluene (5 mL) at room temperature was added to a solution of **17** (15 mg, 1.5 equiv, 0.15 mmol) in toluene (2 mL). The reaction was allowed to stir at room temperature for 2 h, in which time the reaction solution turned orange. The reaction mixture was pumped to dryness to give a pale-yellow solid. The solid was extracted with pentane (2 × 8 mL) and after filtration the pentane filtrant was reduced to half volume and placed at $-35^\circ C$. The pale-yellow crystalline precipitate of the desired compound was isolated by filtration and dried under vacuum to yield **19** (119 mg, 83%). Pale yellow, almost colorless crystals suitable for X-ray analysis were grown by slow evaporation of a pentane solution. 1H NMR ($[D_8]Tol$, 400.1 MHz, 298 K): $\delta = 3.38$ (t, 2H, $^3J_{HH} = 5.9$ Hz, NCH_2), 3.23 (t, 2H, $^3J_{HH} = 6.0$ Hz, NCH_2), 3.15 (s, 3H, OCH_3), 2.83 (s, 3H, NCH_3), 2.29–1.12 (m, 66H, Cy), -7.05 (br, 2H, $\sigma-BH_2$), -12.35 ppm (br, 2H, RuH_2); $^{13}C\{^1H\}$ NMR ($[D_8]Tol$, 100.613 MHz, 298 K): $\delta = 72.73$ (s, OCH_2), 58.92 (s, OCH_3), 52.51 (s, NCH_2), 39.49 (ψ t, CH, Cy), 38.43 (s, NCH_3), 31.43 (s, CH_2 Cy), 28.90 (ψ t, CH_2 Cy), 27.69 ppm (s, CH_2 Cy); $^{31}P\{^1H\}$ NMR ($[D_8]Tol$, 161.975 MHz, 298 K): $\delta = 79.2$ ppm (s); $^{11}B\{^1H\}$ NMR ($[D_8]Tol$, 128.377 MHz, 298 K): $\delta = 47.6$ ppm (br); elemental analysis calcd (%) for $C_{40}H_{80}BNOP_2Ru$: C 62.81, H 10.54, N 1.83; found: C 62.90, H 10.99, N 1.98.

Complex 20: A solution of the diamine–monoborane **18** (64 mg, 1.5 equiv, 0.49 mmol) in toluene (4 mL) was added to a solution of $[RuH_2(\eta^2-H_2)(PCy_3)_2]$ (220 mg, 0.33 mmol) in toluene (10 mL) at room temperature. The reaction was allowed to stir at room temperature for 2 h, in which time the reaction solution turned orange. The reaction mixture was pumped to dryness to give a pale-yellow solid. The solid was extracted with pentane (2 × 8 mL) and after filtration the pentane filtrant was reduced to half volume and placed at $-35^\circ C$. The pale-yellow crystalline precipitate of the desired compound was isolated by filtration and dried under vacuum to yield **20** (119 mg, 46%). Pale yellow, almost colorless crystals suitable for X-ray analysis were grown by slow evaporation of a pentane solution. 1H NMR (C_6D_6 , 400.130 MHz, 298 K): $\delta = 3.17$ (t, 2H, $^3J_{HH} = 7.4$ Hz, NCH_2), 2.80 (s, 3H, NCH_3), 2.35–2.20 (m, 14H, Cy), 2.15 (s, 6H, $N(CH_3)_2$), 1.95–1.20 (m, 58H, $Cy + 3 \times CH_2$), -6.99 (br, 2H, RuH_2B), -12.27 ppm (br, 2H, RuH_2); $^{13}C\{^1H\}$ NMR (C_6D_6 , 100.613 MHz, 298 K): $\delta = 57.77$ (s, NCH_2), 50.88 (s, NCH_2), 45.76 (s, $N(CH_3)_2$), 39.15 (ψ t, Hz, CH Cy), 37.12 (s, NCH_3), 31.11 (s, CH_2 Cy), 28.54 (ψ t, CH_2 Cy), 27.55 (s, $NCH_2CH_2CH_2N$), 27.52 ppm (m, CH_2 Cy); $^{31}P\{^1H\}$ NMR (C_6D_6 , 161.975 MHz, 298 K): $\delta = 79.3$ ppm (s); $^{11}B\{^1H\}$ NMR (C_6D_6 , 128.377 MHz, 298 K): $\delta = 47.4$ ppm (br); elemental analysis calcd (%) for $C_{42}H_{88}BNP_2Ru$: C 63.70, H 10.82, N 3.54; found: C 63.72, H 10.19, N 3.42.

Diamine–monoborane 21: $BH_3 \cdot SMe_2$ (0.27 mL, 5.6 mmol) was added by syringe to a solution of *N,N'*-dimethyl-1,6-hexanediamine (1 mL, 5.6 mmol) in THF (8 mL) at $-78^\circ C$. The reaction solution was allowed to warm to room temperature over 1 h. The reaction mixture was pumped to dryness to yield a white wax as a mixture (839 mg) of **21** and the bis-adduct of $[(CH_2)_3NHMe(BH_3)]$. The mixture was purified by UPLC using a $H_2O/MeOH$ (95:5, v/v) eluent containing 0.1% v/v HCO_2H . The product is detected by UV spectroscopy at 210 nm. The collected fractions are gathered, neutralized with Na_2CO_3 until a pH of 11 is reached, and extracted with CH_2Cl_2 . The organic layer is dried with $MgSO_4$, filtered and evaporated to dryness to give **21** as a white wax. 1H NMR ($CDCl_3$, 300.130 MHz, 298 K): $\delta = 4.16$ (brs, 1H, $NH(BH_3)$), 2.84–2.65 (m, 1H, $CHNHMe(BH_3)$), 2.47–2.60 (m, 1H, $CHNHMe(BH_3)$), 2.52 (t, 2H, $^3J_{HH} = 7.0$ Hz, CH_2NHMe), 2.44 (d, 3H, $^3J_{HH} = 5.7$ Hz, $CH_3NH(BH_3)$),

2.37 (s, 3H, $NHCH_3$), 2.12 (br, 1H, $NHCH_3$), 1.60 (p, 2H, $^3J_{HH} = 7.6$ Hz, $CH_2CH_2NHMe(BH_3)$), 1.45 (p, 2H, $^3J_{HH} = 7.1$ Hz, CH_2CH_2NHMe), 1.36–1.18 ppm (m, 4H, $CH_2 + CH_2$); $^1H\{^{11}B\}$ NMR ($[D_8]THF$, 500.330 MHz, 298 K): $\delta = 1.48$ ppm (br, 3H, BH_3); $^{13}C\{^1H\}$ NMR ($CDCl_3$, 75.468 MHz, 298 K): $\delta = 56.69$ (s, $CH_2NHMe(BH_3)$), 51.66 (s, CH_2NHMe), 41.79 (s, $NH(CH_3)(BH_3)$), 36.27 (s, $N(CH_3)H$), 29.29, 26.68, 26.53, 26.18 ppm (s, CH_2); ^{11}B NMR (C_6D_6 , 96.293 MHz, 298 K): $\delta = -15$ ppm (q, $^1J_{BH} = 99$ Hz); ^{15}N NMR ($[D_8]THF$, 50.717 MHz, 273 K): $\delta = -351$ (d, $^1J_{15NH} = 67$ Hz, $N(H)BH_3$), -357 ppm (br, d, NH). Because of the waxy nature of **21** at room temperature, no elemental analysis could be properly performed.

N-Methylhexylamine borane adduct 25: A 1 M solution of $BH_3 \cdot THF$ in THF (13.2 mL, 1 equiv, 13.19 mmol) was added by syringe to an ethereal solution (5 mL) of *N*-methylhexylamine (2 mL, 1.52 g, 13.19 mmol) at $-20^\circ C$. The reaction solution is left to stir at room temperature for 2 h and the mixture is evaporated to dryness to yield quantitatively **25** as colorless oil. $^1H\{^{11}B\}$ NMR ($[D_8]THF$, 400.130 MHz, 298 K): $\delta = 4.82$ (brs, 1H, NH), 2.71–2.60 (m, 1H, $MeNCHH$), 2.74–2.59 (m, 1H, $MeNCHH$), 2.36 (d, 3H, $^3J_{HH} = 5.6$ Hz, $NHCH_3$), 1.70–1.20 (m, $4 \times CH_2$), 1.30 (brs, 3H, BH_3), 0.89 ppm (t, 3H, $^3J_{HH} = 6.20$ Hz, CH_3 hex); $^{13}C\{^1H\}$ NMR ($[D_8]THF$, 100.613 MHz, 298 K): $\delta = 57.79$ (s, NCH_2), 42.35 (s, NCH_3), 32.62, 27.70, 27.42, 23.55 (s, CH_2), 14.52 ppm (s, CH_3 hex); ^{11}B NMR ($[D_8]THF$, 128.378 MHz, 298 K): $\delta = -14.5$ ppm (q, $^1J_{BH} = 95$ Hz); ^{15}N NMR ($[D_8]THF$, 40.560 MHz, 298 K): $\delta = -350$ ppm (d, $^1J_{NH} = 71$ Hz). Because of the oily nature of **25** at room temperature, no elemental analysis could be properly performed.

Complex 26: A solution of **25** (21 mg, 0.15 mmol) in toluene (5 mL) was added to a solution of $[RuH_2(\eta^2-H_2)(PCy_3)_2]$ (100 mg, 0.15 mmol) in toluene (10 mL) at room temperature. The reaction was allowed to stir at room temperature for 1 h, in which time the reaction solution turns yellow. The toluene was then removed under vacuum, to give a pinkish solid. The solid was taken up in pentane (1 mL) and placed at $-35^\circ C$ overnight. An off-white solid precipitated overnight, and after isolating and drying under vacuum, yielded analytically pure **26** (50 mg, 42%). 1H NMR ($[D_8]Tol$, 400.130 MHz, 298 K): $\delta = 3.06$ (t, 2H, $^3J_{HH} = 7.4$ Hz, $BN(CH_3)CH_2$), 2.76 (s, 3H, NCH_3), 2.13–2.24 (m, 12H, Cy), 2.00–1.10 (m, 62H, $Cy + 4 \times CH_2$ hex), 0.91 (t, 3H, $^3J_{HH} = 6.5$ Hz, CH_3 hex), -7.06 (br, 2H, RuH_2B), -12.38 ppm (br, 2H, RuH_2); $^{13}C\{^1H\}$ NMR ($[D_8]Tol$, 100.613 MHz, 298 K): $\delta = 53.22$ (s, NCH_2), 39.51 (ψ t, CH, Cy), 37.23 (s, NCH_3), 32.79 (s, CH_2 hex), 31.45 (s, CH_2 Cy), 29.50 (s, CH_2 hex), 28.91 (ψ t, CH_2 Cy), 27.90 (s, CH_2 Cy), 27.61 (s, CH_2 hex), 23.54 (s, CH_2 hex), 14.72 ppm (s, CH_3 hex); $^{31}P\{^1H\}$ NMR ($[D_8]Tol$, 161.975 MHz, 298 K): $\delta = 79.4$ ppm (s); $^{11}B\{^1H\}$ NMR ($[D_8]Tol$, 128.377 MHz, 298 K): $\delta = 46.9$ ppm (br); ^{15}N NMR ($[D_8]THF$, 40.560 MHz, 298 K): $\delta = -299$ ppm (s, H_2BM); elemental analysis calcd (%) for $C_{43}H_{86}BNP_2Ru$: C 65.29, H 10.96, N 1.77; found: C 65.52, H 11.62, N 1.65.

CCDC 1056987 (**19**) and CCDC-1056986 (**20**) contain the supplementary crystallographic data. These data can be obtained free of charge by The Cambridge Crystallographic Data Centre.

Computational details

DFT calculations were performed with Gaussian 09 D.01,^[27] with the hybrid B3PW91 functional.^[28] The Ru atom was represented by the relativistic effective core potential (RECP) from the Stuttgart group and the associated basis set augmented by a f polarization function ($\alpha = 1.235$).^[29] The remaining atoms (C, H, B, N, O) were represented by a 6–31G(d,p) basis set.^[30] The P atom was represented by RECP from the Stuttgart group and the associated basis set,^[31] augmented by a d polarization function ($\alpha = 0.387$).^[32] The solvent (thf) influence was taken into consideration through single point

calculations on the gas-phase optimized geometry within the SMD model,^[33] using the ORCA software.^[34] For the solvent calculations the pseudo potential was kept on Ru and all the remaining atoms were treated with tzvpp basis sets.^[35] The influence of the dispersion interactions was taken into account using the D3(bj) correction introduced by Grimme.^[36] The energies reported in this work are Gibbs free energies obtained by summing the electronic energy obtained with the smd model augmented by the gas phase Gibbs correction at 298 K and the D3(bj) contribution. Table S2 in the Supporting Information collects the values of the energy, the Gibbs correction and the dispersion corrections for all the structures optimized.

Acknowledgements

We thank the CNRS and the ANR for support through the ANR program HyBoCat (ANR-09-BLAN-0184).

Keywords: boranes · cyclization · dehydrogenation · density functional calculations · ruthenium · synthetic methods

- [1] a) G. Alcaraz, S. Sabo-Etienne, *Angew. Chem. Int. Ed.* **2010**, *49*, 7170–7179; *Angew. Chem.* **2010**, *122*, 7326–7335; b) H. C. Johnson, T. N. Hooper, A. S. Weller in *The Catalytic Dehydrocoupling of Amine–Boranes and Phosphine–Boranes*, Vol. 49 (Eds.: E. Fernández, A. Whiting), Springer, Heidelberg, **2015**, pp. 153–220.
- [2] A. Staubitz, A. P. M. Robertson, I. Manners, *Chem. Rev.* **2010**, *110*, 4079–4124.
- [3] a) N. C. Smythe, J. C. Gordon, *Eur. J. Inorg. Chem.* **2010**, 509–521; b) A. Staubitz, M. E. Sloan, A. P. M. Robertson, A. Friedrich, S. Schneider, P. J. Gates, J. Schmedt auf der Günne, I. Manners, *J. Am. Chem. Soc.* **2010**, *132*, 13332–13345.
- [4] G. Alcaraz, E. Clot, U. Helmstedt, L. Vendier, S. Sabo-Etienne, *J. Am. Chem. Soc.* **2007**, *129*, 8704–8705.
- [5] Y. Gloaguen, G. Bénac-Lestrille, L. Vendier, U. Helmstedt, E. Clot, G. Alcaraz, S. Sabo-Etienne, *Organometallics* **2013**, *32*, 4868–4877.
- [6] G. Alcaraz, L. Vendier, E. Clot, S. Sabo-Etienne, *Angew. Chem. Int. Ed.* **2010**, *49*, 918–920; *Angew. Chem.* **2010**, *122*, 930–932.
- [7] G. Alcaraz, A. B. Chaplin, C. J. Stevens, E. Clot, L. Vendier, A. S. Weller, S. Sabo-Etienne, *Organometallics* **2010**, *29*, 5591–5595.
- [8] G. J. Kubas, *J. Organomet. Chem.* **2014**, *751*, 33–49.
- [9] C. J. Wallis, H. Dyer, L. Vendier, G. Alcaraz, S. Sabo-Etienne, *Angew. Chem. Int. Ed.* **2012**, *51*, 3646–3648; *Angew. Chem.* **2012**, *124*, 3706–3708.
- [10] H. Tlahuext, F. Santiesteban, E. García-Báez, R. Contreras, *Tetrahedron: Asymmetry* **1994**, *5*, 1579–1588.
- [11] E. J. Corey, R. K. Bakshi, S. Shibata, *J. Am. Chem. Soc.* **1987**, *109*, 5551–5553.
- [12] J. Graton, M. Berthelot, C. Laurence, *Perkin Trans. 2* **2001**, 2130–2135.
- [13] Traces of a bis- σ -aminoborane Ru complex were detected at the end of the reaction along with I regenerated as a result of evolution of dihydrogen (see the Supporting Information of ref. [9]). The bis- σ ligated aminoborane in complex **D** is not easily displaced by dihydrogen (see S34–35 in the Supporting Information).
- [14] R. Custelcean, J. E. Jackson, *Chem. Rev.* **2001**, *101*, 1963–1980.
- [15] A. J. Ashe, J. W. Kampf, C. Müller, M. Schneider, *Organometallics* **1996**, *15*, 387–393.
- [16] D. J. Grant, D. A. Dixon, *J. Phys. Chem. A* **2006**, *110*, 12955–12962.
- [17] G. Alcaraz, S. Sabo-Etienne, *Coord. Chem. Rev.* **2008**, *252*, 2395–2409.
- [18] All the optimized structures discussed in this manuscript are available in a single xyz file in the Supporting Information, allowing the geometries to be viewed.
- [19] R. Dallanegra, A. B. Chaplin, A. S. Weller, *Angew. Chem. Int. Ed.* **2009**, *48*, 6875–6878; *Angew. Chem.* **2009**, *121*, 7007–7010.
- [20] a) W. E. Piers, S. C. Bourke, K. D. Conroy, *Angew. Chem. Int. Ed.* **2005**, *44*, 5016–5036; *Angew. Chem.* **2005**, *117*, 5142–5163; b) T. Stahl, K. Muther, Y. Ohki, K. Tatsumi, M. Oestreich, *J. Am. Chem. Soc.* **2013**, *135*, 10978–10981.
- [21] A. F. Borowski, S. Sabo-Etienne, M. L. Christ, B. Donnadiu, B. Chaudret, *Organometallics* **1996**, *15*, 1427–1434.
- [22] A. Altomare, G. Cascarano, C. Giacovazzo, A. Guagliardi, *J. Appl. Crystallogr.* **1993**, *26*, 343–350.
- [23] G. M. Sheldrick in *SHELX97* (Includes SHELXS97, SHELXL97, CIFTAB)–Programs for Crystal Structure Analysis (Release 97–2), Institut für Anorganische Chemie der Universität, Tammanstrasse 4, D-3400 Göttingen, Germany, **1998**.
- [24] L. J. Farrugia, *J. Appl. Crystallogr.* **1999**, *32*, 837–838.
- [25] in *International Tables for X-ray crystallography*, Vol. IV Kynoch press, Birmingham, England, **1974**.
- [26] L. J. Farrugia, *J. Appl. Crystallogr.* **1997**, *30*, 565–565.
- [27] Gaussian 09, Revision D1, M. J. Frisch, G. W. Trucks, H. B. Schlegel, G. E. Scuseria, M. A. Robb, J. R. Cheeseman, G. Scalmani, V. Barone, B. Menucci, G. A. Petersson, H. Nakatsuji, M. Caricato, X. Li, H. P. Hratchian, A. F. Izmaylov, J. Bloino, G. Zheng, J. L. Sonnenberg, M. Hada, M. Ehara, K. Toyota, R. Fukuda, J. Hasegawa, M. Ishida, T. Nakajima, Y. Honda, O. Kitao, H. Nakai, T. Vreven, J. A. Montgomery, J. E. Peralta, F. Ogliaro, M. Bearpark, J. J. Heyd, E. Brothers, K. N. Kudin, V. N. Staroverov, R. Kobayashi, J. Normand, K. Raghavachari, A. Rendell, J. C. Burant, S. S. Iyengar, J. Tomasi, M. Cossi, N. Rega, J. M. Millam, M. Klene, J. E. Knox, J. B. Cross, V. Bakken, C. Adamo, J. Jaramillo, R. Gomperts, R. E. Stratmann, O. Yazyev, A. J. Austin, R. Cammi, C. Pomelli, J. W. Ochterski, R. L. Martin, K. Morokuma, V. G. Zakrzewski, G. A. Voth, P. Salvador, J. J. Dannenberg, S. Dapprich, A. D. Daniels, Ö. Farkas, J. B. Foresman, J. V. Ortiz, J. Cioslowski, D. J. Fox, Wallingford CT, **2009**.
- [28] a) A. D. Becke, *J. Chem. Phys.* **1993**, *98*, 5648–5652; b) J. P. Perdew, Y. Wang, *Phys. Rev. B* **1992**, *46*, 12947–12954.
- [29] D. Andrae, U. Häußermann, M. Dolg, H. Stoll, H. Preuß, *Theor. Chim. Acta* **1990**, *77*, 123–141.
- [30] P. C. Hariharan, J. A. Pople, *Theor. Chim. Acta* **1973**, *28*, 213–222.
- [31] A. Bergner, M. Dolg, W. Küchle, H. Stoll, H. Preuß, *Mol. Phys.* **1993**, *80*, 1431–1441.
- [32] A. Höllwarth, M. Böhme, S. Dapprich, A. W. Ehlers, A. Gobbi, V. Jonas, K. F. Köhler, R. Stegmann, A. Veldkamp, G. Frenking, *Chem. Phys. Lett.* **1993**, *208*, 237–240.
- [33] A. V. Marenich, C. J. Cramer, D. G. Truhlar, *J. Phys. Chem. B* **2009**, *113*, 6378–6396.
- [34] F. Neese, *WIREs Comput. Mol. Sci.* **2012**, *2*, 73–78.
- [35] A. Schäfer, H. Horn, R. Ahlrichs, *J. Chem. Phys.* **1992**, *97*, 2571–2577.
- [36] a) S. Grimme, S. Ehrlich, L. Goerigk, *J. Comput. Chem.* **2011**, *32*, 1456–1465; b) S. Grimme, J. Antony, S. Ehrlich, H. Krieg, *J. Chem. Phys.* **2010**, *132*, 154104–154119.

Received: April 22, 2015

Published online on July 28, 2015